Cavitation erosion - corrosion behaviour of ASTM A27 runner steel in natural river water

L Tôn-Thât

Institut de Recherche d'Hydro-Québec
Expertises – Mécanique, métallurgie et hydroéolien
1800 boulevard Lionel-Boulet, Varennes (Québec) J3X1S1 – Canada

ton-that.laurent@ireq.ca

Abstract. Cavitation erosion is still one of the most important degradation modes in hydraulic turbine runners. Part of researches in this field focuses on finding new materials, coatings and surface treatments to improve the resistance properties of runners to this phenomenon. However, only few studies are focused on the deleterious effect of the environment. Actually, in some cases a synergistic effect between cavitation erosion mechanisms and corrosion kinetics can establish and increase erosion rate. In the present study, the cavitation erosion-corrosion behaviour of ASTM A27 steel in natural river water is investigated. This paper state the approach which has been used to enlighten the synergy between both phenomena. For this, a 20 kHz vibratory test according ASTM G32 standard is coupled to an electrochemical cell to be able to follow the different corrosion parameters during the tests to get evidence of the damaging mechanism. Moreover, mass losses have been followed during the exposure time. The classical degradation parameters (cumulative weight loss and erosion rate) are determined. Furthermore, a particular effort has been implemented to determine the evolution of surface damages in terms of pitting, surface cracking, material removal and surface corrosion. For this, scanning electron microscopy has been used to link the microstructure to the material removal mechanisms.

1. Introduction

Cavitation erosion is a degradation phenomenon induced by the collapse of bubbles due to pressure fluctuations in turbulent flows. These collapses could generate shock waves and/or micro-jets of the GPa order [1]. In the field of hydraulic machineries, valves or ship propellers, this phenomenon can cause extremely severe damages and the repair costs associated are usually very high. To reduce erosion, several studies have been conducted to develop and characterize materials in order to increase their mechanical properties.

In the past few years, a special effort has been deployed to understand the erosion behaviour of various types of steels like conventional carbon steels [2], austenitic and martensitic stainless steels [3 - 7] as well as stellite alloys [8, 9]. Moreover the solution of coatings has also been explored as well as the surface treatment [10]. Usually in this kind of studies, the electrochemical effect of the environment is neglected. However, a joint interaction of mechanical and chemical factors in a hydrodynamic environment [11, 12] can be involved and modify medium/materials system behaviour.

The purpose of this work is to study the effect of the natural water on the cavitation erosion behaviour of ASTM A27 steel.

2. Experimental approach

2.1. Materials

In the present study, ASTM A27 [13] has been tested. This kind of material has been chosen because of its wide use in hydraulic turbines runners. The chemical composition and the mechanical properties of the tested material are presented in Table 1 and Table 2.

Table 1. Chemical composition of tested materials

Element	**Fe**	**C**	**Si**	**Mn**	**P**	**S**	**Cr**	**Ni**	**Mo**	**Cu**	**Al**	**Sn**
wt.%	97,7	0,28	0,36	0,81	0,02	0,025	0,34	0,12	0,05	0,14	0,073	0,024

Table 2. Mechanical properties of tested materials

Yield strength (MPa)	**Ultimate strength** (MPa)	**Hardness** (HRB)	**A** (%)
350	550	81,5	35

Figure 1 presents the micrographs of ASTM A27 steel. Mean grain size is about 80 μm and the microstructure consists mainly in ferrite, acicular ferrite and pearlite.

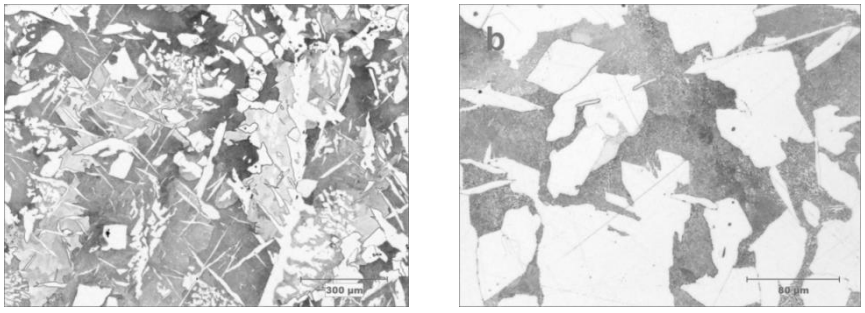

Figure 1. Micrographs of ASTM A27 (Nital 3%)

2.2. Natural river water

The medium that has been used in this work is a naturel river water (NRW). This water is representative of the ones we can find in the south of Quebec. The electrochemical parameters are shown below in Table 3. In this table we can observe that conductivity is quite high for a river water and pH is a little bit alkaline (>7). We can notice the presence of chloride, sulfate and calcium ions in reasonable but non negligible proportions.

Table 3. Natural river water parameters

pH	**Conductivity**	**Cl^-**	**SO_4^{2-}**	**Na^+**	**Ca^{2+}**	**Mg^{2+}**	**Alcalinity**
7.7	277 μS/cm	21 ppm	21 ppm	13 ppm	33 ppm	8 ppm	86 mg $CaCO_3$/L

2.3. Cavitation erosion using vibratory apparatus

In this study, cavitation erosion experiments have been performed in ultrasonic equipment according to ASTM G32 standard [14]. The specimens were held stationary below a vibrating horn at a distance of 0.5± 0.02 mm (indirect method). The frequency of vibration and the peak to peak displacement amplitude of the horn were 20 kHz and 50μm. The experimental apparatus is shown in figure 2

The electrochemical setup was a three-electrode system composed of the working electrode (ASTM A27), Ag/AgCl reference electrode and platinum mesh as a counter electrode. The water bath was a pyrex double walled beaker to prevent any electrochemical reaction and to maintain temperature water at 20±2°C. The setup was connected to a potentiostat/galvanostat to monitor the electrochemical parameters.

After each cavitation erosion and/or corrosion experiment, the surface of the specimen was observed by scanning electron microscopy (SEM) to characterize the evolution with time.

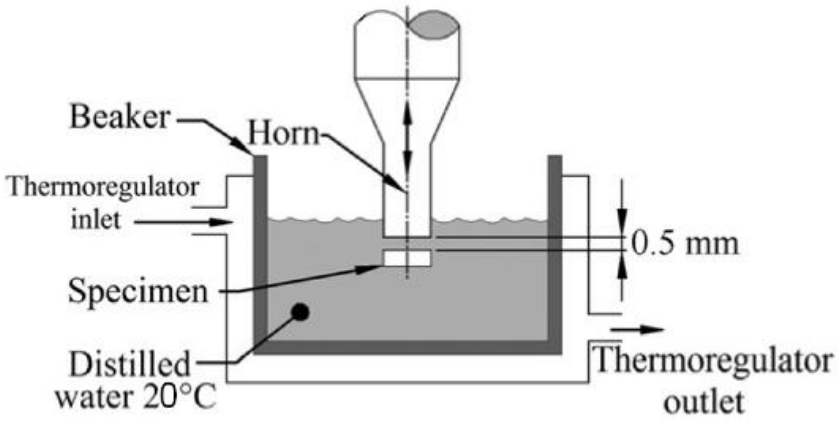

Figure 2. Schematic representation of the cavitation erosion vibratory apparatus

3. Results and discussion

3.1. Erosion resistance

Figure 3 presents the cumulative weight loss as a function of cavitation erosion time for ASTM A27 in distilled water (DW) and natural river water (NRW) for a 650 min period. In these experiments it was evidenced that the cumulative weight loss is a little bit lower in natural river water than in distilled water. However, the difference is very low if we consider the error due to experimental conditions.

Moreover, we can notice that both curves exhibit an incubation period where the weight losses are low, followed by an increase of the cumulative weight losses. The incubation period has been defined as the value obtained from the intersection of a straight extension line of the maximum slope with the time axis. These periods are evaluated at 110 and 115 min respectively in natural river water and distilled water.

After the incubation period the erosion rate (figure 4) increase drastically, demarcating the acceleration period until reaching the maximum erosion rate of 15mg/h and 17.5mg/h respectively in natural river water and distilled water.

In more general terms, these results suggest that natural river water should be less aggressive than distilled water. According to Pourbaix diagram of iron, we can explain this result distortion by the fact that in natural river water (with pH>7), the removed iron particles oxidize in $Fe(OH)_2$, $Fe(OH)_3$, FeO or Fe_2O_3. Actually by this redeposition mechanism, oxides should cover the surface of specimen and induced a deviation during weight measurements. This hypothesis has been confirmed by the presence of a black and orange residual layer on the samples worn surfaces during the experiments in the river water.

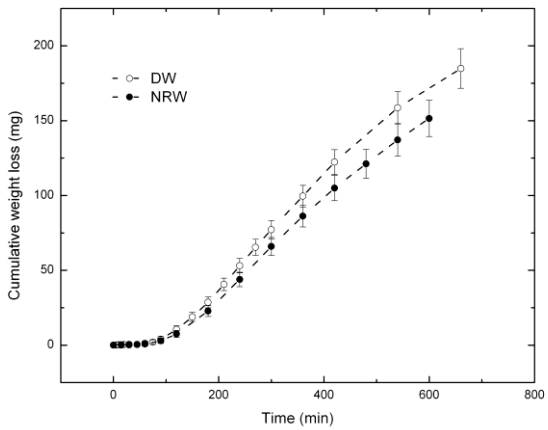

Figure 3. Cumulative weight losses with exposure time

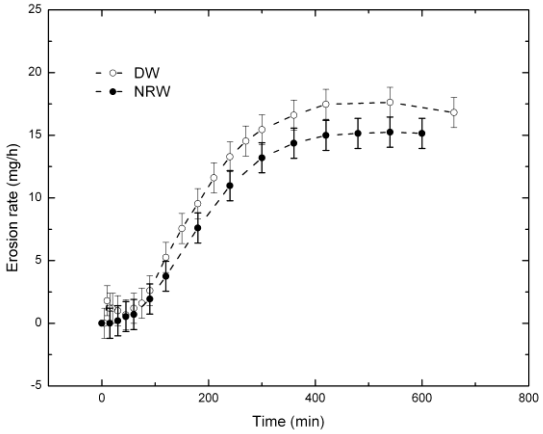

Figure 4. Erosion rate with exposure time

3.2. Corrosion-enhanced cavitation

To get a more advanced understanding of the cavitation erosion mechanism of ASTM A27 steel, it seems relevant to observe degradation during cavitation erosion tests.

Figure 5 presents SEM images of the evolution of worn surface during the test in distilled water. After 15 min of exposure, the surface starts presenting plastic deformation which begins to build up. We can notice deformation steps and a microstructure differentiation between ferrite and pearlite grains. Actually, we clearly distinguish the cementite needles in the pearlite grains. After 30 min, the plastic deformation becomes more severe and grains are drawn. This phenomenon is due to intense formation of slip lines at the grain boundaries. The deformation saturation start to be reached at different place on the surface and some cracks are initiated along the weakest spots on grain boundaries. After 45 min, surface cracks join each other and metal particles are getting free. Then, at 120 min material removal is occurring and the incubation period is finished. The erosion rate starts increasing rapidly. Finally after 240 min, we can observe the ductile fracture with craters and hollows appearing at the surface.

In the case of experiments in natural river water the degradation pattern (figure 6) appears to be different. At the beginning of the test, the first step of damaging consists in corrosion pits formation. Only few places on the surface are affected. We can also notice that these spots are preferential sites for surface dissolution. A slight amount of plastic deformation is also presents on the surface. This plastic deformation intensifies after 30 min. At 60 min, the dissolution process seems to spread and the degradation starts to localise around the existing damages/pits. We can also observe some cracks which are starting to appear. After 120 min the damaging mechanism seems to be a mix between typical cavitation erosion pattern and metal dissolution accompanied with corrosion pitting. Finally at 240 min, dissolution pattern and brittle fracture can be enlightened. The ductile mechanism observed in distilled water is not present in natural river water. The damaging mechanism seems more reproducing a stress corrosion cracking mechanism. In this particular case, the corrosion process localised erosion mechanism in preferential sites.

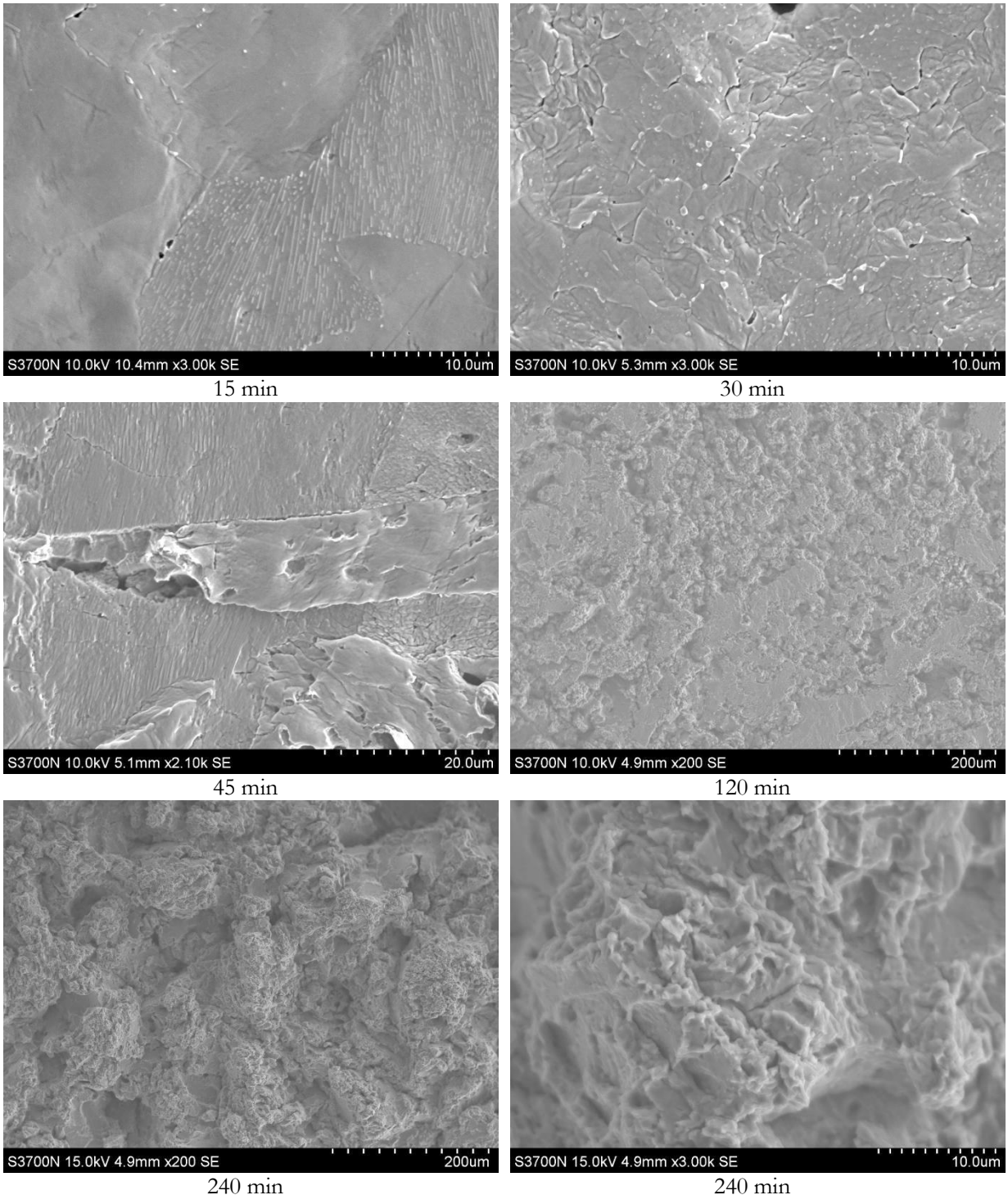

Figure 5. Evolution of ASTM A27 specimen surface during cavitation erosion test in distilled water

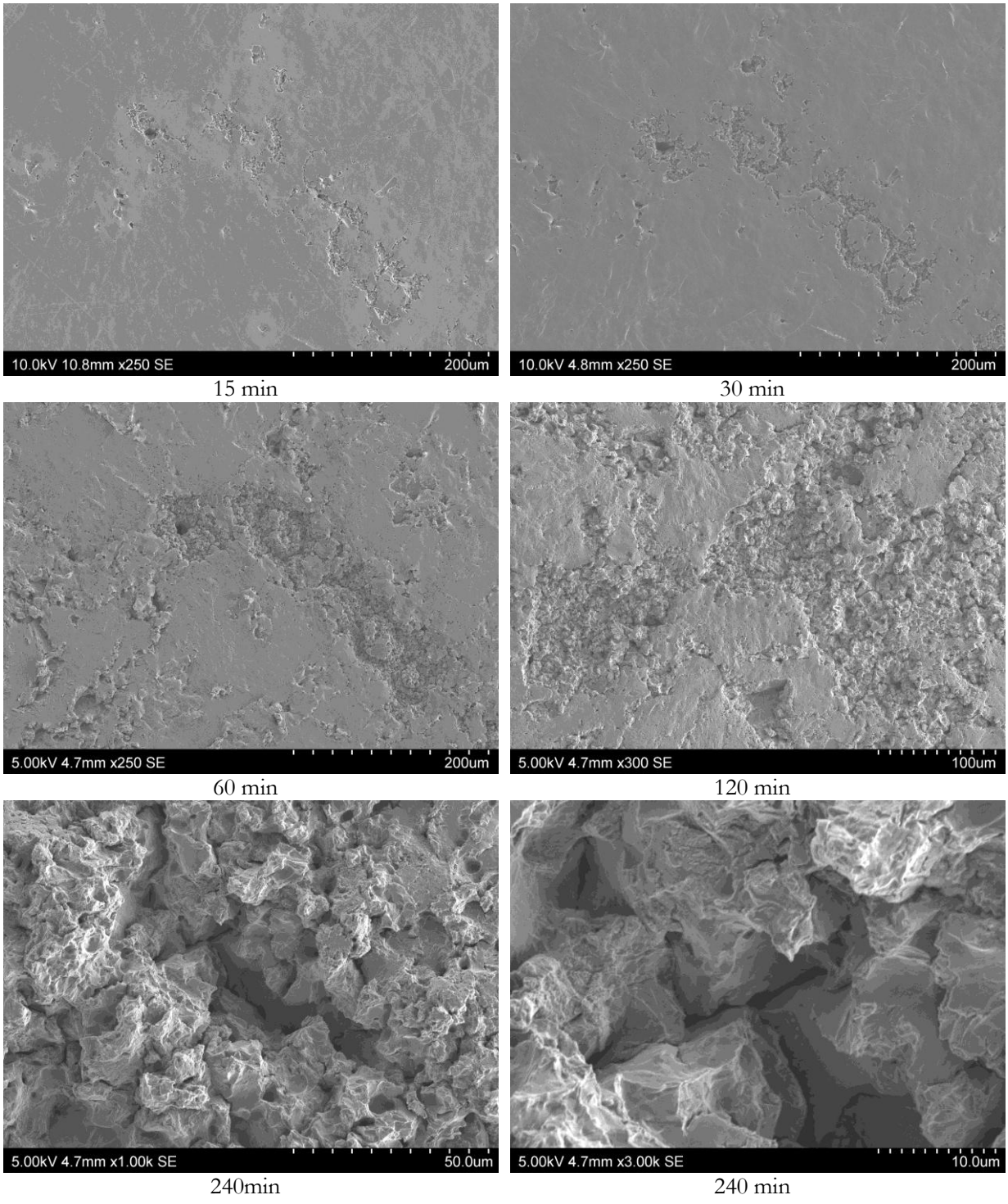

Figure 6. Evolution of ASTM A27 specimen surface during cavitation erosion test in natural river water

3.3. Cavitation-enhanced corrosion

Figure 7 displays the polarization curves of ASTM A27 for Tafel extrapolation in quiescence conditions and under cavitation condition in natural river water. The potentiodynamic anodic and cathodic polarization plots have been obtained by sweeping the potential at a rate of 0.3125 mV/s from -750mV to 0mV.

On this figure, we can observe that the curve representing cavitation condition is shifted towards more positive values by approximately 300mV. A displacement of free corrosion potential toward more anodic value can be related to corrosion film or product removal and to an increase of mass transport under the generation of cavitation bubbles. This kind of effect has also been enlightened by Kwok et al. [12] for mild steel in seawater. Consequently, it is apparent that the corrosion rate is promoted remarkably when cavitation erosion and corrosion are exercised simultaneously.

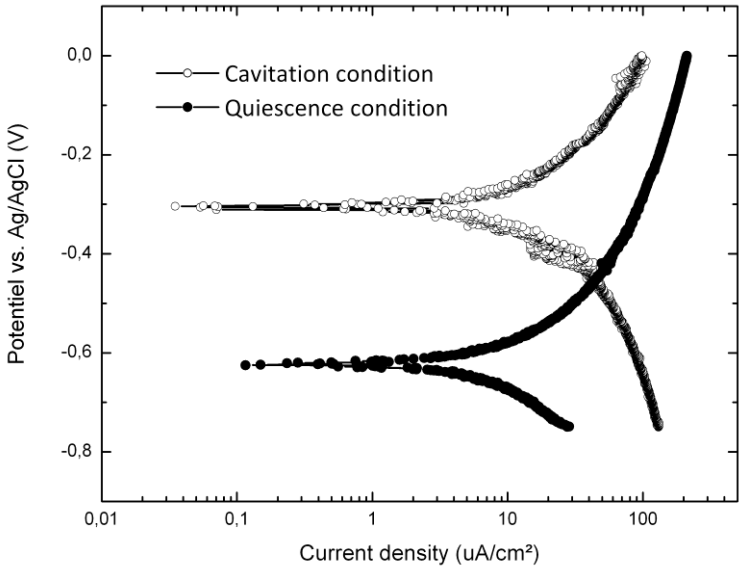

Figure 7. Tafel analysis for ASTM A27 with and without cavitation condition in natural river water

Once the film has been removed, fresh reactive corrosion sites are generated depending on the repassivation rate and the integrity of the film. In this case the repassivation rate is very slow as suggests figure 8. This might be a reason of the low corrosion resistance of mild steels.

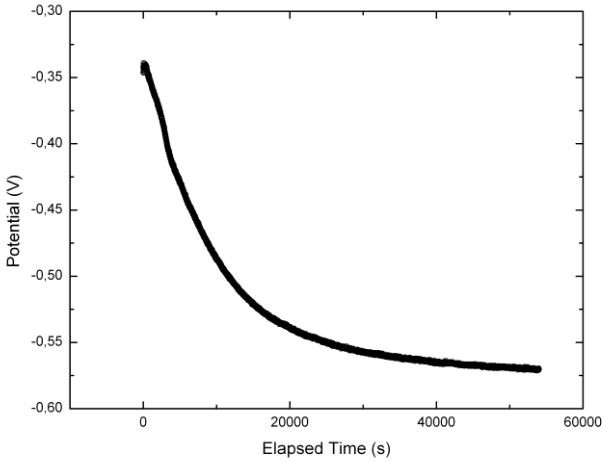

Figure 8. Evolution of open circuit potential of ASTM A27 in natural river water

4. Conclusion

Cavitation erosion - corrosion behaviour of ASTM A27 runner steel in distilled and natural river water has been studied in vibratory apparatus coupled with an electrochemical setup.

The erosion curves shows that in both media the erosion rates are similar. This result is attributed to a surface redeposition mechanism of newly formed oxides in the case of natural river water.

A SEM study shows that corrosion induces a localisation of cavitation damage on preferential sites (pits/dissolved area) in natural river water. This phenomenon has not been observed in non-corrosive medium.

Under the influence of cavitation, the free corrosion potential is shifted in more anodic values. This force the constant values of the potential during the experiment leads to the generation of polarisation currents, which do not occur in quiescence conditions. The material is maintained in an active state.

Acknowledgement
The author wants to acknowledge Hydro-Québec Production for the financial support. He also wants to acknowledge V. Wuelfrath for the excellent technical work he has performed.

References

[1] Vyas B and Preece C 1977 Cavitation erosion of face centered cubic metals Metallurgical Transactions A 8(6) pp 915–923
[2] Hattori S Ishikura R and Zhang Q 2004 Construction of database on cavitation erosion and analyses of carbon steel data Wear 257(9-10) Nov pp 1022–1029
[3] Heathcock C Protheroe B and Ball A 1982 Cavitation erosion of stainless steels Wear 81(2) Oct pp 311–327
[4] Hattori S and Ishikura R 2010 Revision of cavitation erosion database and analysis of stainless steel data Wear 268(1-2) pp 109 – 116
[5] Santa J Blanco J Giraldo J and Toro A 2011 Cavitation erosion of martensitic and austenitic stainless steel welded coatings Wear 271(9-10) pp 1445–1453
[6] Tôn-Thât L 2010 Experimental comparison of cavitation erosion rates of different steels used in hydraulic turbines In IAHR Symposium
[7] Tôn-Thât L 2012 Cavitation erosion behaviour of high strength steels Proceedings of the 8th International Symposium on Cavitation Singapore
[8] Heathcock C Ball A and Protheroe B 1981 Cavitation erosion of cobalt-based stellite® alloys cemented carbides and surface-treated low alloy steels Wear 74(1) Dec pp 11–26
[9] Hattori S and Mikami N 2009 Cavitation erosion resistance of stellite alloy weld overlays Wear 267(11) pp 1954 – 1960
[10] Singh R Tiwari S K and Mishra S K 2010 Cavitation Erosion in Hydraulic Turbine Components and Mitigation by Coatings: Current Status and Future Needs Journal of Materials Engineering and Performance
[11] Wood R J K Wharton J A Speyer A J and Tan K S 2002 Investigation of erosion–corrosion processes using electrochemical noise measurements Tribol Int 35 pp 631–641
[12] Kwok C T Cheng F T Man H C 2000 Synergistic effect of cavitation erosion and corrosion of various engineering alloys in 3.5% NaCl solution Mat Sci Eng A290 pp 55–73
[13] ASTM International 2013 Standard Specification for Steel Castings, Carbon, for General Application A27/A27M
[14] ASTM International 2010 Standard test method for cavitation erosion using vibratory apparatus G32-10